J Mater Sci (2007) 42:1856–1863
DOI 10.1007/s10853-006-0898-6

Optical properties of silver-doped aluminophosphate glasses

J. A. Jimenez · S. Lysenko · G. Zhang · H. Liu

Received: 24 April 2006 / Accepted: 28 August 2006 / Published online: 9 January 2007

Abstract Silver-doped aluminophosphate glasses were prepared by the melt-quenching technique in which silver nanoparticles (NP) of different sizes were embedded upon heat treatment. Optical absorption and photoluminescence spectroscopy were used to study the optical properties of the material before and after thermal processing. Photoluminescence (PL) experiments revealed a broadband emission observed around 420 nm for the non-heat treated samples with a luminescence decay showing a bi-exponential behavior. Temperature dependence PL studies showed a thermal quenching effect on the broadband emission. Our data suggests that the emission is due to single Ag^+ ions. Optical absorption measurements performed on the heat treated samples allowed for particle size estimation and the evaluation of the thermal stability of the glass system and its attributes as a host for NP inclusion. The nanocomposite showed a dip in the broadband emission of silver ions ascribed to absorption of Ag^+ ions luminescence by surface plasmons in the silver particles.

Introduction

Metal-doped materials have been the subject of increasing interest due to their prospective utilization for photonic applications [1–8]. Special attention has been given to noble metal nanoparticles (NP) [3–5, 8] due to their remarkable optical properties owing to the surface plasmon resonance (SPR), the nanometer scale feature which is the origin of the observed colors in metal colloids [9]. The SPR is regarded as the collective excitation of the conduction band electrons. The electric field of an incident light beam polarizes these electrons with respect to the heavier ionic cores. A restoring force develops at the NP surface with the resulting excitation of the free electrons oscillations. This surface plasmon absorption shows distinctive features (e.g. frequency, shape, width) that are directly connected to the composition and morphology of the NP [10–12].

Potential applications for composite materials consisting of spherical metal NP embedded in a glass matrix call for appropriate glass hosts capable of allowing the controlled precipitation of metallic particles with relative simplicity of preparation. In addition, the optical properties of small metal particles, which are strongly dependent on the structural and geometric parameters of the particles (e.g. size, shape, composition) are ultimately determined by the preparation process [10, 13, 14]. There are several preparation techniques that can be employed for metal NP incorporation into a dielectric host: melt-quenching, sol–gel, sputtering, and ion exchange and implantation. Among these, the melt-quenching technique offers the advantages of using conventional systems and allowing a high flexibility of composition, thus facilitating the production of glasses with special properties [15]. For instance, it has been demonstrated by Uchida et al. [14] that a $50MO–50P_2O_5$ (M = Ba, Ca) mol.% glass system prepared by melt-quenching comprises a high

S. Lysenko · G. Zhang · H. Liu (✉)
Department of Physics, University of Puerto Rico, Mayagüez, PR 00681, USA
e-mail: hliu@uprm.edu

J. A. Jimenez
Department of Chemistry, University of Puerto Rico, Mayagüez, PR 00681, USA

metal solubility so a high concentration of small metal NP can be integrated into the matrix by heat treatment processes. Moreover, modification of the network former, for example by adding together a less acid one such as Al_2O_3, would lead to improved thermal properties and control of NP formation during heat treatment.

A comprehensive characterization capable of exploring the optical properties of this type of materials as a function of thermal processing is central from both fundamental and technological standpoints. In such a ground, optical absorption and photoluminescence (PL) spectroscopy have proved to be valuable tools in studying the evolution of the optical properties of silver-doped glasses through thermal treatment and the subsequent formation of nanoparticles [2]. Additionally, even though metal NP-doped glasses have been extensively studied in regard to NP optical properties [3–5, 9, 10, 14–16], reports on PL studies of these materials are still limited [1, 2, 6–8]. In this work, we prepared a silver-doped aluminophosphate glass system by melting in which Ag NP of various sizes were precipitated depending on heat treatment conditions. The optical properties of the material before and after thermal processing were studied by optical absorption and conventional and laser-excited PL spectroscopy. Luminescence measurements have revealed a broadband emission from silver ions around 420 nm for the silver-doped glass without thermal treatment. The elucidation of the nature of the silver emitting states was achieved through optical absorption measurements in conjunction with temperature dependence PL and emission decay experiments. Optical absorption measurements performed on the heat treated samples allowed us to detect Ag NP and estimate their mean particle size, which in turn permitted the evaluation of the thermal stability of the glass system and its attributes as a host for NP inclusion. Heat treatment leads to a change in the optical properties of the material as the surface plasmon peak of the silver particles is positioned close to 420 nm resulting in the absorption of silver ions luminescence by the particles.

Experimental

Sample preparation

Aluminophosphate glasses of composition P_2O_5:Al_2O_3:CaO:SrO:BaO with an additional 4 mol.% of Ag_2O and SnO (in relation to the network former P_2O_5) were prepared by conventional melt and heat treatment processes. The preparation method is similar to the one described in reference [14] which produces spherical silver particles with a size distribution of about only a few nanometers. The batch materials were melted at 1140 °C for 15 min. and immediately quenched. Subsequent heat treatment within the 450–600 °C range was done for different time intervals in order to obtain composite samples with Ag NP of various mean particle size. Samples were cut and polished for spectroscopic measurements. Final thicknesses were ~0.4 mm. Samples used in the present study include: the glass host (glass system without silver and tin); the glass host containing tin (SnO added); non-heat treated silver-doped glasses (i.e. without NP, containing the redox chemicals Ag_2O and SnO); and the Ag NP glass composites obtained by various heat treatment conditions of the silver-doped glasses.

Spectroscopic measurements

Absorption spectra were collected in the 200–800 nm range. Dual-beam configuration was used in order to detect silver ions absorption with the glass host and tin-containing host as references. PL spectroscopy was carried out by both conventional and laser excitation methods. Room temperature (298 K) conventional PL was performed in an ISA SPEX Fluoromax-2 spectrofluorometer equipped with a Xe lamp. Emission spectra were collected at 355 nm excitation for the glass host (glass system without silver and tin), the glass host containing tin, non-heat treated silver-doped samples (containing both redox chemicals without NP) and Ag NP glass composites. The excitation spectrum for the non-heat treated silver-doped glass was collected by monitoring the 420 nm broadband emission. Laser-excited PL was obtained by using the third harmonic radiation of a 20 ps Nd:YAG laser at 355 nm. The decay curve for the silver-doped glass was acquired at room temperature with a TEKTRONIX Oscilloscope. Laser-excited PL for the Ag NP composites was obtained at room temperature. Low temperature (~10 K) emission spectra were collected for the glass host and a non-heat treated silver-doped glass with samples mounted in the coldfinger of a closed-cycle refrigerator. The PL temperature dependence of the non-heat treated silver-doped glass was observed in the 10–280 K range while keeping other conditions constant in order to make possible the comparison of PL intensities (only PL spectra intended for emission intensity comparison).

Particle size estimation

It is widely accepted that for mean particle radii $R < 10$ nm, no significant shift in the SPR peak is observed [8, 10, 16]. In this size regime, the so-called quasi-static approximation of the Mie theory holds and a $1/R$ size dependence of the full width at half maximum (FWHM) of the absorption band is observed [10]. Hence, assuming a narrow size distribution within this size region, mean particle radii were approximated by Hayakawa et al. [8], as $R = \upsilon_f/\Delta\omega_{1/2}$, where R is the particle radius, υ_f is the Fermi velocity of the metal and $\Delta\omega_{1/2}$ is the FWHM for the absorption band in units of angular frequency. For larger particles, the SPR band is significantly red shifted and subsequently becomes broadened making the $1/R$ approximation no longer suitable for particle size estimation [12, 14, 16]. Under such circumstances, a better approximation is achieved by taking into account higher order multipole modes in the Mie relation for the extinction coefficient K(cm^{-1}), which includes both absorption and scattering [10, 16]. Arnold and Borders [16] considered the contribution of higher order resonance modes other than the electric dipole one in evaluating the Mie theory for small silver particles embedded in a transparent medium. They built a theoretical curve for spectral position of SPR absorption maximum as a function of particle radius. Based on comparison of the theoretical curve with experiments where the mean size of glass-embedded silver NP was determined by electron microscopy, they were able to justify the use of the SPR peak spectral position for assigning a particle radius in the 10.0–50.0 nm range. It is observed by Arnold and Borders [16] that for silver particles in the $R = 1.0$–10.0 nm range, the SPR peak position is nearly the same and therefore it is difficult to estimate particle size in this region by this approach. A 10.0 nm radius would correspond to a peak positioned at about 409 nm, indicating that this approximation is best suited for SPR peaks located at longer wavelengths.

Our heat treated samples show the strong SPR absorption band characteristic of spherical silver particles dispersed in a dielectric host with spectral peaks located at wavelengths longer than 409 nm, suggesting mean particle radii larger than 10 nm [16]. In fact, the SPR band widths, which appear quite narrow, are consistent with particles over ~4.0 nm in radius [8]. Also, a red shift of the SPR band was observed with increasing heat treatment temperature and holding time as described in the following section. It should be noted that SPR peak position can also be affected by electrodynamic interactions between closely spaced NP, for instance when aggregation between particles takes place [10]. However, from the extent of the absorption coefficients we estimate particle volume fractions in our samples to be in the order of 10^{-5}, concentrations at which it is less likely for such aggregation effects to become appreciable [10, 14]. Hence, SPR peak position was used for estimating mean particle size of Ag NP in our composites on the basis of comparison with the theoretical curve from Arnold and Borders [16] (estimated mean radii are shown in the figures). In the present investigation, particle size estimation is employed in the analysis of the thermal behavior and particle formation capacity of the glass system.

Results and discussion

Photoluminescence and absorption of non-heat treated aluminophosphate glasses

Laser-excited PL spectra collected at 10 K and 355 nm excitation are shown in Fig. 1a, b for samples of the glass host and the non-heat treated silver-doped glass, respectively. The host shows a weak broadband emission as observed in (a). In fact, emission spectra collected at 355 nm excitation at room temperature in the Fluoromax for the host and the tin-containing host yielded similar profiles with the same feature (not shown). As shown in Fig. 1b a broadband emission with a maximum around 420 nm is obtained for the non-heat treated silver-doped glass. Since the host has a weak structureless emission as observed in Fig. 1a, the emission band around 420 nm is clearly due to the ionic silver. We proceed to elucidate the nature of the silver emitting states in this section.

Figure 2 shows the excitation spectrum obtained for the silver-doped glass by monitoring the 420 nm broadband emission. The emission maximum is positioned at an excitation wavelength around 275 nm. The inset shows the absorption profile of the glass in the 220–340 nm range as recorded in dual-beam mode with the glass host as the reference. An absorption band centered at about 275 nm is observed. Since a measurement with the host that contains tin as reference yielded the same result (spectrum not shown), it is evident that this band is mainly due to silver ions absorption. Paje et al. [17] observed a broad absorption band centered at about 260 nm for a silver-doped silicate glass prepared by the melt-quenching technique, but since they also observed the same peak in the host glass, they did not attribute it to silver. In contrast, Borsella et al. [18] performed spectroscopic investigations on a range of silver concentrations in

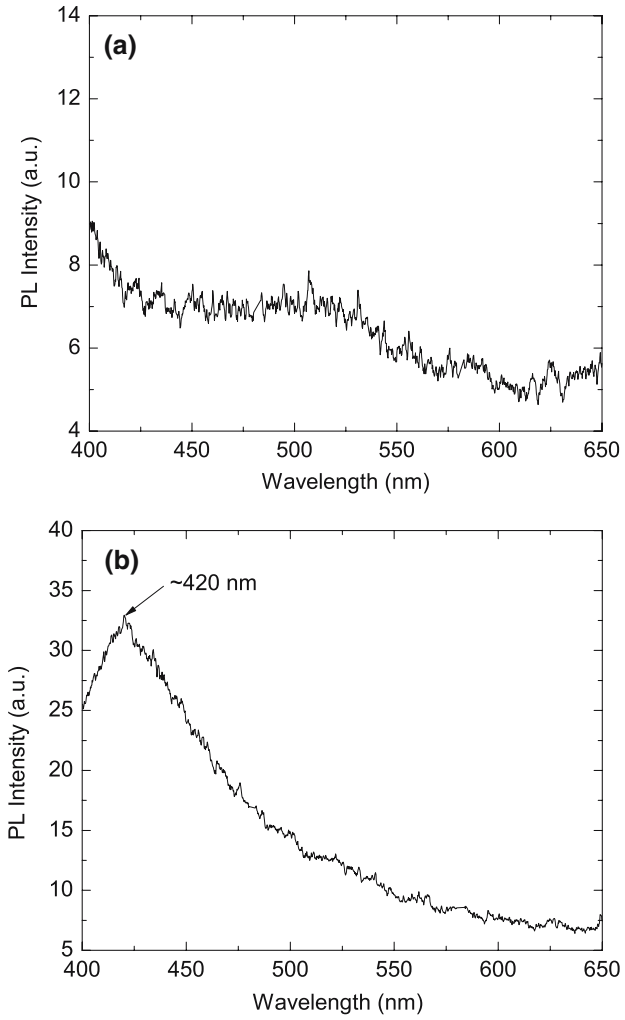

Fig. 1 Emission spectra collected at 10 K with laser excitation at 355 nm for: (**a**) glass host which shows a weak structureless emission; (**b**) non-heat treated silver-doped glass which shows a broadband emission with a maximum at about 420 nm

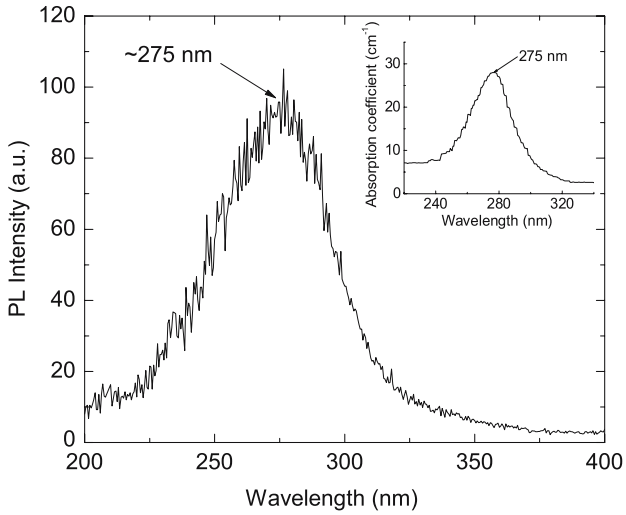

Fig. 2 Excitation spectra of the non-heat treated silver-doped glass collected at room temperature with detection wavelength set at 420 nm; excitation maximum shown at about 275 nm. The inset shows the silver ions absorption peak at 275 nm as recorded in the dual-beam configuration with the glass host as reference

soda-lime glass prepared by the ion-exchange process and observed an absorption band at about 268 nm for silver ions. The absorption was ascribed to transitions involving the promotion of an electron from the $4d^{10}$ ground state to some levels in the $4d^9\ 5s^1$ configuration. Although, these transitions are parity-forbidden, they are partially allowed in a solid due to vibrational coupling. Thus, it is reasonable to ascribe the silver ions absorption in our glass peaked at about 275 nm to the $4d^{10} \rightarrow 4d^9\ 5s^1$ parity-forbidden transitions. The ground state of the free silver ion is $^1S_0$ whereas the lowest electronic excited states in order of increasing energy are $^3D_3$, $^3D_2$, $^3D_1$ and $^1D_2$. These excited states are further split by local order in the glass with the consequent inhomogeneous broadening due to long range disorder. The question then arises as to the nature of the emitting states responsible for the observed luminescence which are inherently related to the absorbing species undergoing the $4d^{10} \rightarrow 4d^9\ 5s^1$ parity-forbidden transitions. Our results from temperature dependence measurements on the broadband emission intensity were found to be a key feature in this elucidation.

Figure 3 shows the temperature dependence of the broadband emission in the silver-doped glass. The displayed spectra for 10, 130 and 280 K show a decrease in luminescence intensity with increasing temperature. Meijerink et al. [19] carried out PL studies of Ag^+ in glassy SrB_4O_7 and observed an emission band centered at about 420 nm. Their temperature dependence studies showed an increase for the PL intensity of the band with increasing temperature. They concluded that this behavior was due to a more effective energy transfer from isolated Ag^+ to Ag^+ pairs at high temperatures. They explained that increasing the temperature leads to an increase in spectral overlap between the isolated Ag^+ emission band and the Ag^+ pair excitation band due to thermal broadening of both bands. Thus, they attributed the 420 nm emission to Ag^+ pairs. On the other hand, Borsella et al. [18] conducted a study of silver ions in soda-lime glass and observed an emission at about 435 nm with an intensity that increased with silver concentration. They also found a decrease in emission intensity as temperature increased, so the 435 nm band was not assigned to energy transfer processes from isolated ions to pairs. In addition, they

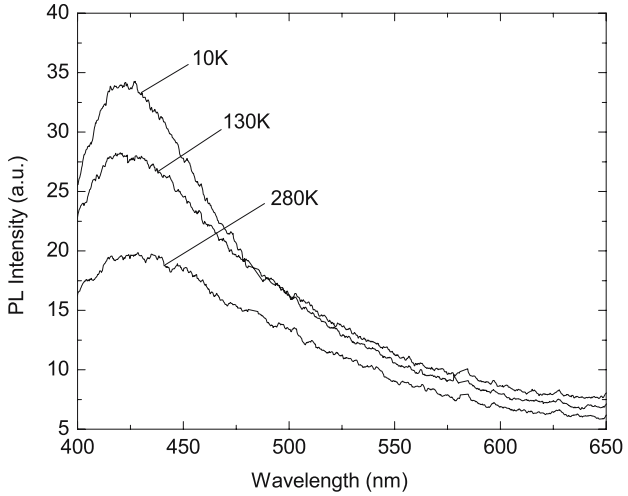

Fig. 3 Emission spectra of the non-heat treated silver-doped glass collected at different temperatures with laser excitation at 355 nm. Emission intensity decreases with increasing temperature

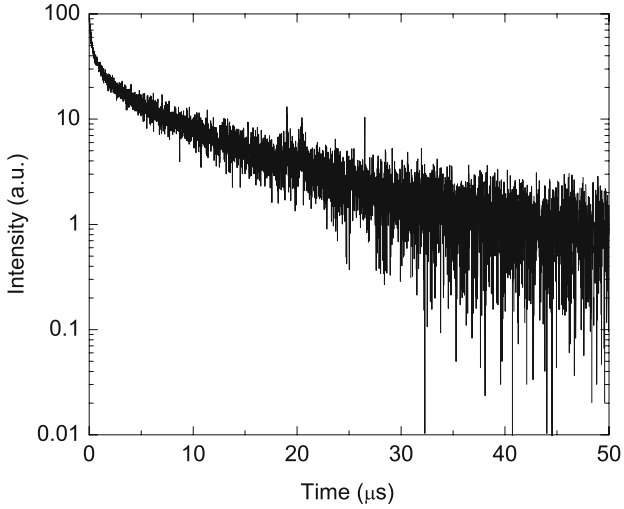

Fig. 4 Emission decay of the non-heat treated silver-doped glass collected at room temperature with laser excitation at 355 nm and detection wavelength set near the top of the broadband at 430 nm

observed an emission at about 330 nm at low concentrations of silver which was quenched at high concentrations (1% molar). This quenching effect was related to an excitation transfer mechanism between electronic states of the same silver ion (self-quenching), rather than to an energy transfer between ions in proximity. Moreover, their excitation spectra with detection wavelength at 435 nm peaked at about 266 nm, close to the observed silver absorption peak at about 268 nm. Therefore, they ascribed the higher energy emission at 330 nm to spin-allowed transitions from the $^1D_2$ state to the $^1S_0$ ground state and the 435 nm band to spin-forbidden transitions from the ^3D level to the $^1S_0$ ground state in single Ag^+ ions. They emphasized the stronger singlet character acquired due to singlet-triplet state mixing at higher silver concentrations which is evidenced by the appearance of the absorption peak at 268 nm. Their assignment to Ag^+ ions turned out to be in agreement with a previous study by Mesnaoui et al. [20] who investigated the luminescence of Ag^+ ions in a phosphate glass system of the type $Ag_xNa_{1-x}PO_3$. This group observed an emission around 400 nm that showed an excitation peak at about 275 nm for a silver concentration up to 10% and assigned it to isolated Ag^+ ions. Accordingly, the thermal quenching effect that we observed for the broadband emission suggests that single Ag^+ ions are the source of this luminescence.

The decay curve shown in Fig. 4 was obtained for the silver-doped glass at 355 nm excitation with the detection wavelength set near the top of the broadband emission at 430 nm. A bi-exponential curve fitting yields estimated fast and slow components of 1.3 and 11.7 μs, respectively. A four-level system has been described [18] to explain this type of luminescence decay of Ag^+ ions, where laser excitation immediately populates the excited singlet state (level 4) which can relax nonradiatively to two other metastable states (levels 2 and 3) lying close to each other. After a relatively short time period, level 4 is emptied and the system behaves as a three-level one in which relaxation from level 3 is fast, while that from level 2 is slower. In this context, the fast (1.3 μs) and slow (11.7 μs) components of Ag^+ ions emission that we report are likely to be related to relaxation from metastable upper (level 3) and lower (level 2) states, respectively, to the ground state (level 1).

Summarizing, in our experiments we observed the matching of the excitation maximum for the 420 nm emission with the silver absorption peak at about 275 nm and a thermal quenching effect on silver ions luminescence. In agreement with [18] and [20], the former indicates a strong singlet character of the silver emitting states while the latter points toward single Ag^+ ions and not to $(Ag^+)_2$ silver pairs as the source of the observed luminescence. In addition, no higher energy PL emission was observed, which is consistent with the relatively high concentration of silver we are dealing with (4 mol.% Ag_2O). The observed dynamical behavior for silver ions luminescence shown in Fig. 4 is also similar to those reported for single Ag^+ ions [18]. All these being considered, we ascribe the 420 nm broadband emission to single Ag^+ ions spin-forbidden transitions of the type $^3D_J \rightarrow {}^1S_0$ ($J = 3, 2, 1$) possessing a strong singlet character.

Heat treatment of the silver-doped aluminophosphate glasses

Absorption spectroscopy and thermal behavior of the glass system

The most conspicuous consequence of heat treatment on the optical properties of the material under study is the SPR. Absorption profiles for the heat treated samples can be observed in Fig. 5a–c. Figure 5a shows spectra for glass samples heat treated at 500 °C for 6, 9 and 12 h with SPR peaks at 413, 416 and 419 nm, respectively. With increasing holding time at 500 °C, a slight red shift of 3 nm is observed in SPR peak position between samples, implying an estimated 2 nm increase in radius among each. In regard to absorption intensity, a strong increase is observed with holding time. Theory predicts that for particles larger than 10 nm in radius, not only the SPR band red shifts but absorption intensity decreases [10]. The size increase for such larger particles would not lead to an increase in resonance intensity provided the density of the particles is comparable [16]. This is because, according to the Mie theory [10, 16], the strength of the absorption coefficients is also proportional to the volume fraction of the particles in the matrix, also referred to as the filling factor, *f*, the ratio of the volume occupied by the NP in the host to the total volume of the material. Hence, according to the size estimation method used [16], our data suggests that the increase in holding time at 500 °C supports increasing particle concentrations. Samples heat treated for 6 and 9 h, with estimated mean radii around 14 and 16 nm, show SPR band widths with FWHM of about 30 and 28 nm, correspondingly. Although slight, this band width decrease is in accord with a particle size increase in the region close to 10 nm [10]. On the other hand, a noticeable difference in band width can be observed between those samples processed for 9 and 12 h with estimated mean radii of 16 and 18 nm and FWHM of about 28 and 37 nm, respectively. Several factors can be taken into account as potential contributors to such behavior. First, it is expected for particles above a certain size threshold exceeding 10 nm that the FWHM increases with increasing particle size [10]. Hence, the increase in band width among these two samples would be in accord with an increase in mean particle size in the estimated size region. We should note however, that a broadened particle size distribution would also lead to a broadened absorption band. In fact, broader distributions are likely evident with longer holding times due to continuous nucleation and growth where the first nucleated crystals have the largest sizes [21].

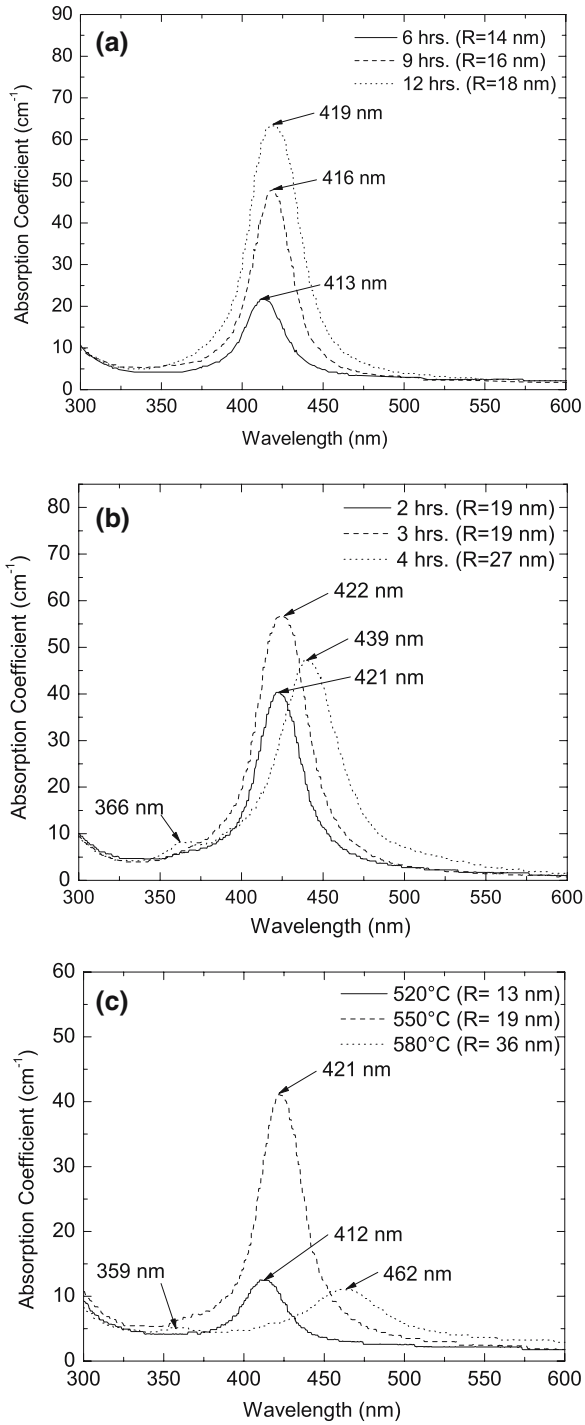

Fig. 5 Absorption spectra of Ag NP-doped glasses obtained by various heat treatment conditions (absorption maxima and estimated radii shown): (**a**) heat treated at 500 °C; (**b**) heat treated at 550 °C; (**c**) heat treated for 2 h

Thus, it seems likely that the broadening is affected by a broader particle size distribution as well.

Spectra presented in Fig. 5b correspond to glass samples heat treated at 550 °C during 2, 3 and 4 h with SPR peaks positioned at 421, 422 and 439 nm,

respectively. For this higher temperature, larger particle sizes were estimated, as observed with the sample processed for 2 h, for which the estimated mean radius is 19 nm. An additional hour at 550 °C, i.e. 3 h of holding time, lead to a 1 nm red shift in the SPR maximum. Accordingly, no significant particle growth is estimated relative to the sample heat treated for 2 h since the estimated mean radius is about 19 nm for both. We observe a slight increase in FWHM among these two samples from about 32 to 37 nm corresponding to 2 and 3 h of processing, respectively. Since we estimate mean particle sizes to be comparable, the broadening in SPR width seems to be related to a broader size distribution. Also, the absorption intensity increase among these samples suggests an increased particle volume fraction. A great red shift was observed for the sample processed at 550 °C during 4 h with SPR peak at 439 nm, corresponding to an estimated mean radius of 27 nm. This sample shows a second peak at ~366 nm ascribed to the quadrupolar plasmon excitation characteristic of relatively large NP [14]. It also shows a further broadening of the SPR band, with FWHM of about 43 nm. In this case, this could be due not only to a broader particle size distribution but also to the increase in mean particle size. The decrease in absorption intensity for this sample relative to the one processed for 3 h is also consistent with a particle size increase.

The greatest red shifts (and thus particle size increase) were obtained for increasing temperatures during isochronal (2 h of holding time) heat treatments as can be observed in Fig. 5c. These glass samples were heat treated at temperatures of 520, 550 and 580 °C and showed SPR peaks at 412, 421 and 462 nm corresponding to estimated mean particle radii of 13, 19 and 36 nm, respectively. Among samples heat treated at 520 and 550 °C, a difference in SPR peak position of 9 nm is observed, implying a particle radius increase of about 6 nm. For the samples processed at 550 and 580 °C, the SPR peak red shifts an additional 41 nm corresponding to a particle radius increase of about 17 nm among these. The larger particle size of the sample processed at 580 °C is also evidenced by the appearance of the quadrupole resonance absorption at ~359 nm. Raising the temperature from 520 to 550 °C did not cause an appreciable increase in band width since this spectra show FWHM of about 30 and 32 nm, respectively. This is in accord with the estimated mean particle radii for the corresponding samples since the broadening due to increase in particle size becomes more evident the farther from the 10 nm threshold [10, 16]. However, at 580 °C, we do observe a significant broadening for the sample which shows a FWHM of about 53 nm. We recall that at the estimated mean particle size of Ag NP in this sample it is likely to observe such broadening [10, 16]. However, a broader size distribution would also be a contributor for such behavior. A significant increase in absorption intensity is observed at 550 °C in relation to 520 °C. Here, mean particle radius increases from about 13 to 19 nm for the 520 and 550 °C samples, respectively. Within this size range, theory predicts that an increase in particle size is accompanied by a decrease in resonance intensity [10]. Nevertheless, Uchida et al. [14] reported an increase in resonance peak intensity with increasing particle size for Ag NP with radii below 15 nm for Ag NP embedded in a phosphate glass system similar to ours. In this scenario, we can not entirely discard the possibility of an absorption intensity increase associated with particle size effects especially in view of particle size estimation. On the other hand, the enhancement of transport processes in the amorphous material with increasing temperature might provide favorable conditions for an increase in particle volume fraction. For the sample processed at 580 °C, absorption intensity decreased considerably relative to the 550 °C sample and is comparable to the one heat treated at 520 °C. Herein, a considerable influence of particle size is expected for such large silver particles leading to decreased absorption coefficients [16].

Photoluminescence of the nanocomposite

Figure 6 shows the emission spectrum collected at room temperature for a silver NP composite with SPR peak at 423 nm. It shows a dip in the broadband emission with a minimum at about the SPR maximum in the NP. It should be recalled that the broadband emission of silver ions is situated around 420 nm for the non-heat treated glasses, which is close to the plasmon absorption peak of the silver particles. This would represent a favorable condition for radiative energy transfer from the emitting silver ions to the silver particles which possess a high absorption coefficient. Additionally, after optical pumping of the electronic system in silver nanoparticles, energy exchange processes leading to relaxation and return of the system to equilibrium occur in the femtosecond to picosecond timescales [9]. Thus, the fact that the lifetimes of the emitting states in Ag^+ ions were found to be in the microsecond timescale, also supports an effective energy transfer process. Hence, the effect of the aggregated atomic silver is to absorb the luminescence emitted by single Ag^+ ions in the glass host.

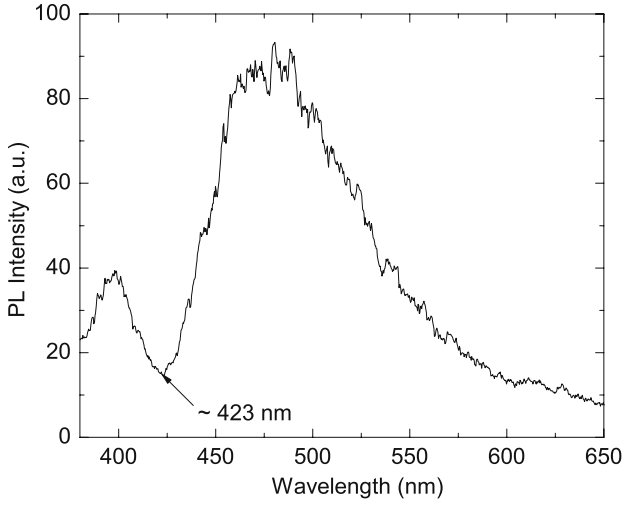

Fig. 6 Emission spectrum of Ag NP-doped glass with SPR peak at 423 nm collected at room temperature with laser excitation at 355 nm. A dip is observed with a minimum at about the SPR maximum in the NP

Conclusions

The optical properties of the silver-doped aluminophosphate glass system were studied before and after thermal processing by optical absorption and conventional and laser-excited PL spectroscopy. For the non-heat treated glass, a broadband emission around 420 nm was observed for silver ions which showed a thermal quenching effect as observed in temperature dependence studies. The excitation spectrum for the emission band showed a maximum around 275 nm which was found to match the absorption peak for silver ions. A bi-exponential curve fitting of the measured emission decay yielded fast and slow components of 1.3 and 11.7 μs, most likely corresponding to relaxation from upper and lower metastable states in Ag^+ ions, respectively. Our data indicates that the broadband emission is due to $^3D_J \rightarrow {}^1S_0$ ($J = 3, 2, 1$) spin-forbidden transitions in single Ag^+ ions which posses a strong singlet character due to singlet-triplet state mixing.

Optical absorption measurements performed on the heat treated samples have demonstrated the capability of the aluminophosphate glass system for allowing a controlled precipitation of spherical silver nanoparticles with estimated mean particle radii in the 10–40 nm range. It was observed that particle growth is better promoted at temperatures $T \geq 550$ °C. Holding time is more likely to increase particle concentration provided the temperature is not too high, i.e. $T < 550$ °C; for higher temperatures it can sustain significant particle growth. The photoluminescence of the material after heat treatment is characterized by a dip in the broadband emission of silver ions corresponding to the dipole resonance mode of Ag NP. The dip in the emission spectrum of the nanocomposite is ascribed to absorption of Ag^+ ions luminescence by surface plasmons in the silver particles.

The effectiveness of the glass system in supporting various particle sizes and volume fractions presents the opportunity to study phenomena related to optical dynamics and local field enhancements. Forthcoming research will follow this direction.

Acknowledgements This work was supported by US-DOD-W911NF-04-1-0019, NASA-NCC5-518 and ARO-DAAD19-02-1-0298.

References

1. Portales H, Matarelli M, Montagna M, Chiasera A, Ferrari M, Martucci A, Mazzoldi P, Pelli S, Righini GC (2005) J Non-Cryst Solids 351:1738
2. Gangopadhyay P, Kesavamoorthy R, Bera S, Magudapathy P, Nair KGM, Panigrahi BK, Narasimhan SV (2005) Phys Rev Lett 94:47403
3. Liao H, Lu W, Yu S, Wen W, Wong GKL (2005) J Opt Soc Am B 22:1923
4. Karthikeyan B, Thomas J, Philip R (2005) Chem Phys Lett 414:346
5. Hamanaka Y, Nakamura A, Hayashi N, Omi S (2003) J Opt Soc Am B 20:1227
6. Almeida RM, Marques AC, Ferrari M (2003) J Sol–Gel Sci Technol 26:891
7. Strohhöfer C, Polman A (2002) Appl Phys Lett 81:1414
8. Hayakawa T, Selvan ST, Nogami M (1999) J Non-Cryst Solids 259:16
9. Voisin C, Del Fatti N, Christofilos D, Valleé F (2001) J Phys Chem B 105:2264
10. Kreibig U, Vollmer M in ''Optical Properties of Metal Clusters'' (Springer, Berlin, 1995)
11. Kelly KL, Coronado E, Zhao LL, Schatz GC (2003) J Phys Chem B 107:668
12. Sönnichsen C, Franzl T, Wilk T, von Plessen G, Feldman J (2002) New J Phys 4:93
13. Link S, El-Sayed MA (2003) Annu Rev Phys Chem 54:331
14. Uchida K, Kaneko S, Omi S, Hata C, Tanji H, Asahara Y, Ikushima AJ, Tokisaki T, Nakamura A (1994) J Opt Soc Am B 11:1236
15. Yamane M and Asahara Y, in ''Glasses for Photonics'' (Cambridge University Press, UK, 2000)
16. Arnold GW, Borders JA (1977) J Appl Phys 48:1488
17. Paje SE, Llopis J, Villegas MA, Fernández Navarro JM (1996) Appl Phys A 63:431
18. Borsella E, Battaglin G, García MA, Gonella F, Mazzoldi P, Polloni R, Quaranta A (2000) Appl Phys A 71:125
19. Meijerink A, van Heek MME, Blasse G (1993) J Phys Chem Solids 54:901
20. Mesnaoui M, Maazaz M, Parent C, Tanguy B, Le Flem G (1992) Eur J Sol State Inorg Chem 29:1001
21. Fokin VM, Zanotto ED, Yuritsyn NS, Schmelzer JWP (2006) J Non-Cryst Solids 352:2681